Hindawi Publishing Corporation
Advances in Meteorology
Volume 2016, Article ID 4741390, 11 pages
http://dx.doi.org/10.1155/2016/4741390

Research Article

Interannual Variation of the Surface Temperature of Tropical Forests from Satellite Observations

Huilin Gao,[1] Shuai Zhang,[1] Rong Fu,[2] Wenhong Li,[3] and Robert E. Dickinson[2]

[1]*Zachry Department of Civil Engineering, Texas A&M University, College Station, TX 77840, USA*
[2]*Department of Geological Sciences, Jackson School of Geosciences, University of Texas at Austin, Austin, TX 78712, USA*
[3]*Earth and Ocean Sciences, Nicholas School of the Environment, Duke University, Duke, NC 27708, USA*

Correspondence should be addressed to Huilin Gao; hgao@civil.tamu.edu

Received 15 December 2014; Revised 8 May 2015; Accepted 17 May 2015

Academic Editor: Thomas Van Niel

Land surface temperatures (LSTs) within tropical forests contribute to climate variations. However, observational data are very limited in such regions. This study used passive microwave remote sensing data from the Special Sensor Microwave/Imager (SSM/I) and the Special Sensor Microwave Imager Sounder (SSMIS), providing observations under all weather conditions, to investigate the LST over the Amazon and Congo rainforests. The SSM/I and SSMIS data were collected from 1996 to 2012. The morning and afternoon observations from passive microwave remote sensing facilitate the investigation of the interannual changes of LST anomalies on a diurnal basis. As a result of the variability of cloud cover and the corresponding reduction of solar radiation, the afternoon LST anomalies tend to vary more than the morning LST anomalies. The dominant spatial and temporal patterns for interseasonal variations of the LST anomalies over the tropical rainforest were analyzed. The impacts of droughts and El Niños on this LST were also investigated. Differences between early morning and late afternoon LST anomalies were identified by the remote sensing product, with the morning LST anomalies controlled by humidity (according to comparisons with the National Centers for Environmental Prediction (NCEP) reanalysis data).

1. Introduction

Accurate and reliable observations are essential for characterizing and understanding climate variations and long term change. *In situ* observations in the tropics are sparse, and their uncertainty tends to be larger than that in the northern hemisphere mid-latitudes. Although several versions of gridded data have been interpolated from *in situ* meteorological measurements (e.g., [1]) and made available at a global scale, discrepancies arise amongst these datasets due to their different spatial averaging techniques, treatment of gaps in the data, and the number of stations used by different analyses [2]. Observations over tropical forests are extremely sparse, especially for the time period before the late 1970s [3]. Surface warming in these regions could substantially change the regional and global terrestrial exchange of carbon with the atmosphere [4–6]. *In situ* measurements, which represent the surface air temperature at 2 m above the surface, are mostly located over grass or bare ground and differ by as much as 3 to 5 K from the land surface temperature (LST) of a tropical forest canopy [7]. Such large differences could confound accurate detection of changes in LST (which is also referred to as the canopy skin temperature, in the case of rainforests) and subsequently hinder evaluation of global climate models (GCMs) over tropical forests.

The most advanced (and now the most commonly used) LST measurements are those from the Moderate Resolution Imaging Spectroradiometer (MODIS), which resides on each of the NASA Earth Observation System (EOS) satellites—terra and aqua (since 1999 and 2002, resp.). However, MODIS measurements are limited to clear sky conditions and provide few samples over the tropical forests when skies are cloudy and/or rainy [7, 8]. To address this problem, Gao et al. [7] developed an empirical algorithm to provide the forest canopy skin temperature during all weather conditions using the Advanced Microwave Scanning Radiometer for the Earth Observing System (AMSR-E). In addition, about 30-year microwave data have been collected from passive radiometers

such as the Scanning Multichannel Microwave Radiometer (SSMR, 1978 to 1987), the Special Sensor Microwave/Imager (SSM/I, 1987 to present), and the Special Sensor Microwave Imager Sounder (SSMIS, 2003 to present). The LST based on these passive microwave retrievals from different radiometers, if calibrated against each other, could potentially allow us to examine changes of canopy skin temperature in the tropical forests since the late 1970s—the period when the global air temperature increase has become rapid and attributable to anthropogenic forcing [9, 10].

This work uses the microwave derived all weather LST product to investigate the interannual variability of the canopy skin temperature over tropical forests. The 19 GHz polarized brightness temperatures were collected by F13 SSM/I and F17 SSMIS. The F13 SSM/I was in service from May 1995 to November 2009, while F17 SSMIS has been collecting data from December 2006 to present. We focus on studying LST anomalies from January 1996 to December 2012 over both the Amazon and the Congo basin rainforests. An intersatellite calibration of the 19 GHz polarized brightness temperatures during the overlapping period between F13 SSM/I and F17 SSMIS was conducted to maintain consistency between the two data sources.

The objective of this study is to answer the following questions:

(1) What are the dominant spatial and temporal patterns for interannual variations of canopy skin temperature over tropical rainforests?

(2) How would droughts and El Niños affect the LST over these two regions?

(3) How different are the interannual changes of early morning (6 a.m.) and late afternoon (6 p.m.) LST anomalies? Are these differences physically reasonable?

We concentrate on the Amazon and Congo basins. Section 2 introduces the satellite data and the intercalibration method, as well as the other data sources used in this study; Section 3 shows the results and analyses over the Amazon forest; Section 4 investigates the LST anomalies over the Congo basin forest; and Section 5 summarizes results and draws conclusions.

2. Data and Methodology

2.1. SSM/I and SSMIS Satellite Data. The first SSM/I sensor (F08) was launched in 1987 by the Defense Meteorological Satellites Program (DMSP). Since then, a series of SSM/I and SSMIS sensors (F11, F13, F15, F16, F17, and F18) have been launched consecutively to measure atmosphere, ocean, and terrain microwave brightness temperatures at near real time. Flying in a polar orbit, these sensors provide both vertically and horizontally polarized microwave data at 3 frequencies—19.35, 37.0, and 85.5 GHz—and horizontally polarized data at 22.2 GHz. The ascending and descending equatorial crossing times for the satellites used in this study (i.e., F13 and F17) are very near 6 p.m. and 6 a.m. This paper obtains the brightness temperatures from data collected by the NOAA/NASA SSM/I Pathfinder Program made available from the National Snow and Ice Data Center (NSIDC). We used the level 3 Equal-Area Scalable Earth-Grid (EASE-Grid) brightness temperatures ([11], http://nsidc.org/data/docs/daac/nsidc0032_ssmi_ease_tbs.gd.html). The data are daily, separated by ascending and descending passes, and consist of gridded values at 25 km resolution. However, since the daily observations cannot cover the entire globe, there is typically one overpass on every other day for a given location. Consequently, the average number of observations per pixel per month is approximately 15. We further interpolated the EASE-Grid data into 0.25° resolution grids.

The input orbital brightness temperature data from NSIDC were ingested via the Remote Sensing Systems (RSS) software [12], with the mode for sensor intercalibrations turned off. We chose to study the 17-year period from January 1996 to December 2012, to cover significant climate variability—including events such as the 1997 to 1998 strong El Niño and the 2005 and 2010 droughts over the Amazon. The F17 observed horizontally and vertically polarized brightness temperatures ($T_{b,h}$ and $T_{b,v}$) were calibrated according to their counterpart F13 measurements. The process contains three steps: (1) averaging the ascending (and descending) brightness temperatures ($T_{b,h}$ and $T_{b,v}$) from daily to monthly for both the F13 and the F17 observations; (2) deriving a linear relationship between F13 and F17 for each pixel during the overlapping period of the two satellites (i.e., from 2007 to 2008); and (3) calibrating F17 observations from 2009 to 2012 based on the relationship established in step 2.

2.2. SSM/I LST over the Tropical Rainforest. A global land cover map derived from MODIS was used to select the tropical forests over the Amazon basin and Congo basin. The LST for these areas was retrieved using 19.35 GHz polarized brightness temperatures and an algorithm developed by Gao et al. [7]. The general concept of the LST microwave retrieval algorithm lies in the combined use of two equations, as outlined below. The first equation is based on the brightness temperature definition as follows:

$$T_s = \frac{T_{b,h}}{\varepsilon_h}, \tag{1}$$

where T_s is the LST, $T_{b,h}$ is the horizontal brightness temperature, and ε_h is the horizontal emissivity. The value for ε_h can be inferred from the Polarization Ratio (PR), which is defined as $\mathrm{PR} = T_{b,h}/T_{b,v}$. To establish the empirical ε_h-PR relationship during a training period, ε_h was calculated as the ratio between MODIS LST and SSM/I $T_{b,h}$.

As described in Gao et al. [7], the quality controlled MODIS LST data during a dry month in July 2002 were selected as the training data. The training domain was the forested area within the entire Amazon basin, from 20°S to 13°N latitude and 82°W to 34°W longitude. Since the empirical relationship is independent of observation time, the same relationship was used for estimating LST both in the morning and in the afternoon. The empirical relationship is shown as

$$\varepsilon_h = 1.0038 \times \mathrm{PR} \times \mathrm{PR} - 0.1226 \times \mathrm{PR} + 0.0799. \tag{2}$$

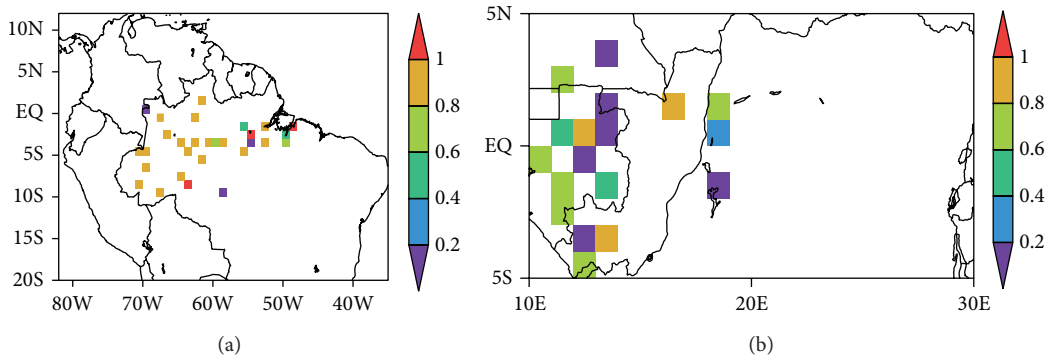

FIGURE 1: The temporal coverage of rain gauges within each 1°× 1° pixel with the results represented as a fraction of the total time duration from 1996 to 2006 over (a) the Amazon rainforests and (b) the Congo rainforests.

Once the ε_h-PR relationship was established, passive microwave based LST could be estimated from $T_s = T_{b,h}/\varepsilon_h$.

In the study by Gao et al. [7], the passive microwave LST was validated using *in situ* temperature measurements (at the satellite overpass time) from 12 meteorological stations under all weather conditions over the Amazon forests. The correlation coefficient and Root Mean Square Error (RMSE) during the cloudy/rainy days were 0.68 and 1.7 K, respectively. The passive microwave LST during the cloudy/rainy days actually outperformed the remotely sensed LST during the clear days (both from the microwave sensor and from MODIS).

For each day from January 1, 1996, to December 31, 2012, LST values were calculated for the ascending and descending orbits, respectively. To eliminate the nonforested areas in this study, a 1°× 1° mask which extracted the rainforests was applied to the SSM/I brightness temperature data. The mask was derived from the MODIS land cover classification map. The daily LSTs were then averaged for each month to smooth out random uncertainties from the daily data. We further calculated the temperature anomalies for each month for both the descending/morning and the ascending/afternoon orbits. In order to focus on variations at seasonal and interannual levels, the monthly anomalies were smoothed using a 3-month moving average.

2.3. Rainfall Data from the Global Precipitation Climatology Centre (GPCC). We used monthly precipitation from the Global Precipitation Climatology Centre (GPCC), at 1°× 1° resolution, to assist the analysis. This precipitation data is derived from *in situ* measurements obtained from rain gauge networks [13]. Figure 1 shows the distribution of rain gauges and the temporal availability within each 1°× 1° pixel, from 1996 to 2006 over the two rainforests studied. It appears that the Amazon has more evenly distributed stations than the Congo basin and that most of the gauges have collected data over the entire period studied. A comparison of rainfall datasets by Juarez et al. [14] suggests that GPCC data agree well with the Tropical Rainfall Measurement Mission (TRMM) product over tropical South America. The number of rain gauges over the Congo basin is very limited, and they tend to be concentrated at the edge of the forest. Additionally, most of these instruments only collected data over a short period. Therefore, in the following sections, the comparison of rainfall with the LST anomalies is limited to the Amazon. The GPCC data is also used for calculating the Standard Precipitation Index (SPI [15]) to investigate the relationship between LST anomalies and drought in Section 3. Recommended by the World Meteorological Organization as a standard to characterize meteorological droughts [16], SPI is a probability index that has been used in many studies for abnormal wetness and dryness conditions [15, 17–20].

2.4. Data from the National Center for Environmental Prediction (NCEP) Reanalysis. Monthly surface air temperature and specific humidity data from the National Center for Environmental Prediction (NCEP) reanalysis [21] from 1996 to 2012 were employed for analyzing their linkage to the remotely sensed LST anomalies over the Amazon rainforests in the next section.

3. Results over the Amazon Tropical Rainforests

3.1. Time Series of the LST Anomalies Interannual Variations. Figure 2(a) indicates a good agreement between the remotely sensed morning LST anomalies and the NCEP surface air temperature, but this is not the case in the afternoon. This is because the LST anomalies from remote sensing physically represent the canopy skin temperature—which is more influenced by nighttime longwave radiation and thus has a stronger connection to the humidity and temperature of the overlying atmosphere and cloud base [22]. In contrast, the afternoon LST anomalies tend to be higher than the air temperature when it is warm and lower than the air temperature when it is cold.

Figure 2(b) shows that the LST anomalies have a negative correlation with SPI, with correlation coefficients of −0.73 and −0.36, for the afternoon and morning data, respectively. The higher correlation of LST anomalies with SPI in the afternoon is as expected, because the daytime clouds associated with rainfall reduce surface solar flux and a larger fraction of solar heating goes into latent fluxes (e.g., [23]).

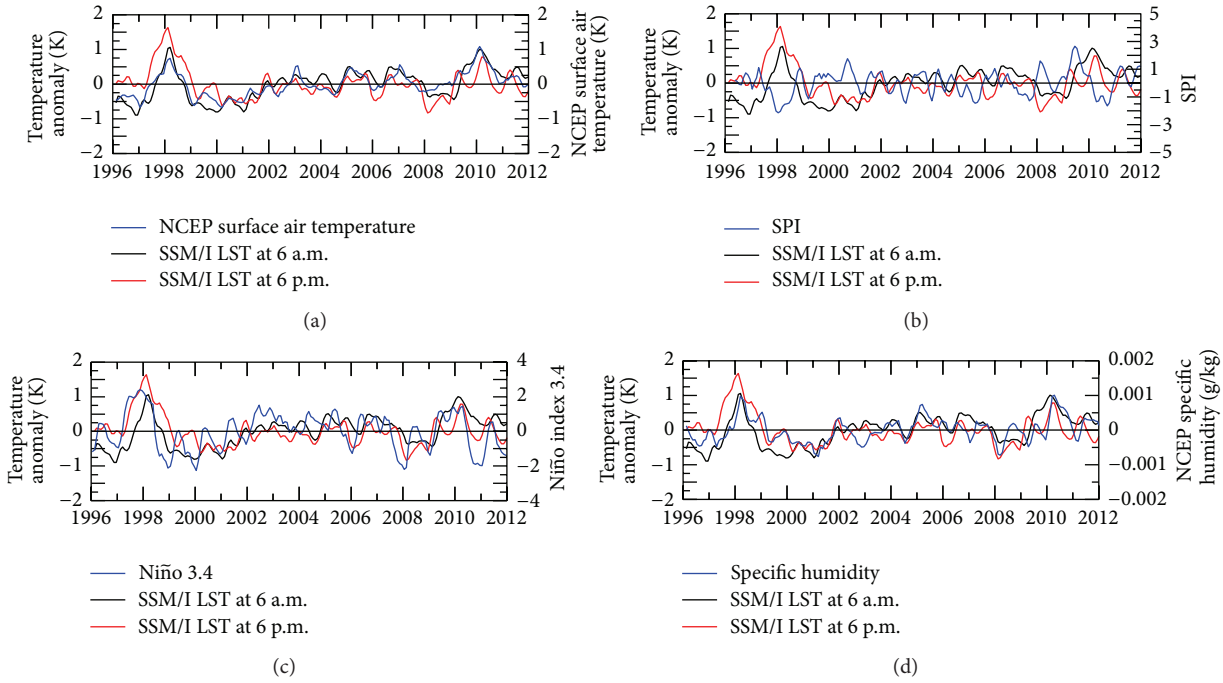

Figure 2: Comparison between time series of the domain averaged temperature anomalies of remotely sensed LST (at 6 a.m. and 6 p.m.) over Amazon rainforests with the following: (a) NCEP surface air temperature, (b) SPI, (c) Niño 3.4 index, and (d) NCEP specific humidity.

The interannual variation of climate over Amazon rainforests is mainly triggered by the El Niño Southern Oscillation (ENSO), an anomaly of sea-surface temperature (SST) and atmospheric pressure patterns over the equatorial Pacific that is commonly characterized by SST anomalies in the Niño 3.4 region (5°N-5°S, 170°W-120°W). Thus the Niño 3.4 index [24] is used to characterize ENSO. Figure 2(c) compares time series of both morning and afternoon LST anomalies with this Niño 3.4 index. They both strongly respond to the El Niño event of 1997-1998, but the 2002-2003 El Niño was too weak to impact the LST anomalies significantly. The 2010 drought shows a larger impact on the LST anomalies at 6 a.m. than at 6 p.m. The LST anomalies lag Niño 3.4 by 3-4 months (with lag correlations of 0.8 for morning LST anomalies and 0.7 for afternoon LST anomalies), consistent with the results reported by Trenberth et al. [25].

Figure 2(d) indicates a strong connection between the remotely sensed morning LST anomalies and the specific humidity from the NCEP reanalysis. The response of the canopies—as well as the response of their carbon flux—to droughts is related to canopy skin temperature. During the 17 years studied, three major drought events occurred over the Amazon: the 1998 drought triggered by a strong El Niño and the 2005 and 2010 droughts, each caused by an unusually long period of anomalously low rainfall. Figure 3 compares the spatial distributions of temperature anomalies for representative months of the three drought years, March 1998, March 2010 (peak of the 1997/98 and 2010 drought, resp.), and January 2005 (peak of the 2005 drought) in the morning and in the afternoon. The LST has strong positive anomalies in 1998 (especially in the afternoon), but little impact from the drought in 2005 when the rainfall deficit was not particularly large (as shown in Figure 2(b)). This difference indicates—as expected—a dependence of LST anomalies on soil moisture. The greater shortage of soil moisture in 1998 is also confirmed by the SPI. The 2010 drought has shown a much larger impact on LST than does the 2005 drought, but its anomalies are slightly smaller than those in 1998. The spatial patterns from 1998 and 2010 are also very different.

3.2. Spatial Patterns of Interannual Variation by Season. It is difficult to obtain reliable spatial patterns of LST anomaly change with the sparse *in situ* measurements in the Amazon rainforests. In contrast, spaceborne remote sensing regularly provides spatially homogeneous measurements that are only limited by the length of their time series in determining the spatial patterns of the interannual changes of LST (and their relation to changes of rainfall). In this section, we examine the spatial patterns of interannual rainfall anomalies in the four different seasons (MAM, JJA, SON, and DJF) during the morning and afternoon separately.

The spatial patterns of the LST anomaly standard deviation are shown in Figures 4 and 5 for the morning and afternoon, respectively. In both morning and afternoon, variations of LST anomalies during the dry season (JJA) are smaller than those during the wet season (DJF). Furthermore, these variations are smallest at locations farthest from the equator, mainly because of the decreased variability of the rainfall. Variations are larger in the afternoon than in the morning, due to the greater variability of incident solar radiation.

The Empirical Orthogonal Function (EOF) is a statistical tool for identifying the dominant patterns of the correlated

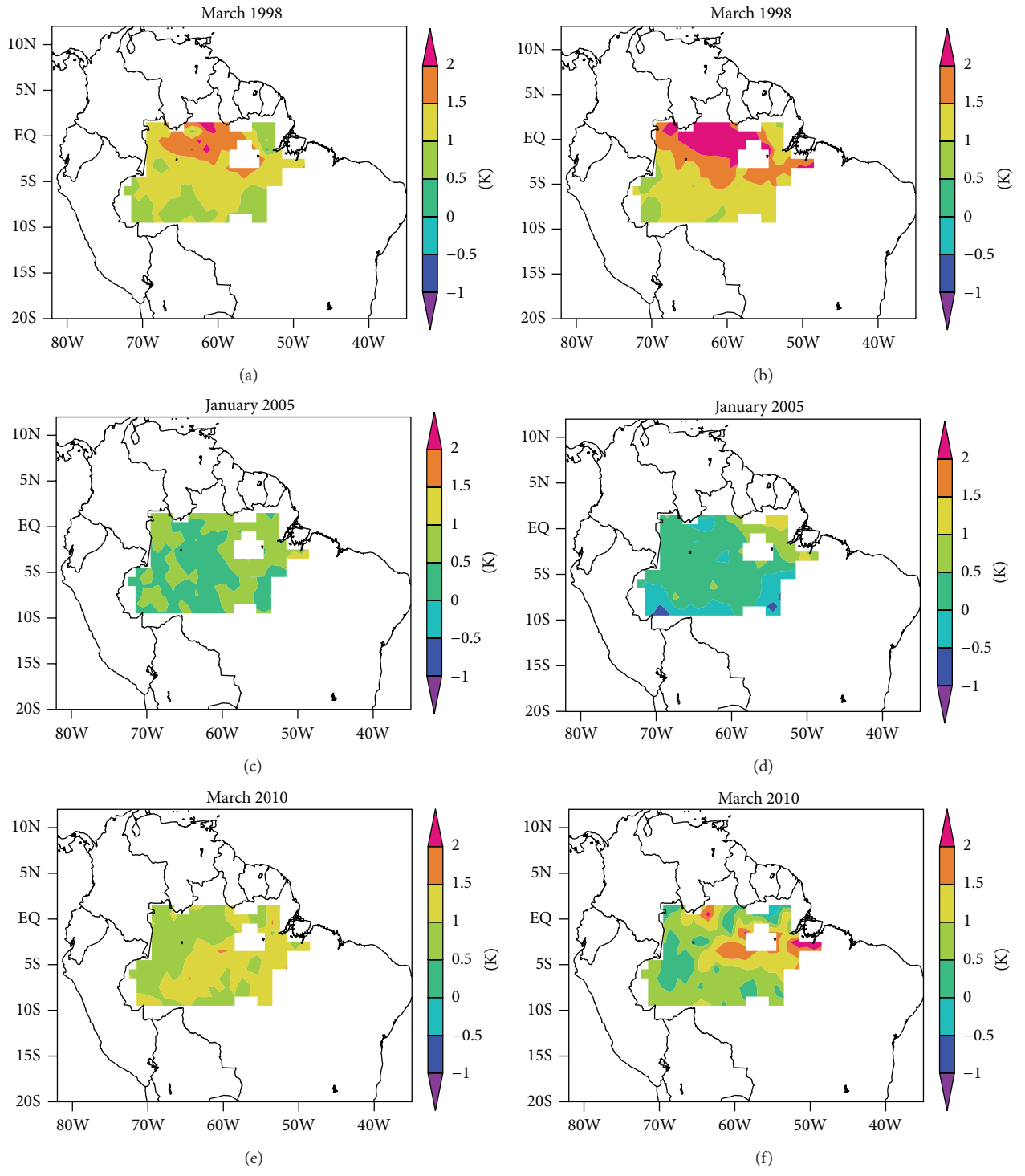

Figure 3: Spatial distribution of the remotely sensed LST anomalies over Amazon rainforests during three drought events in March 1998, January 2005, and March 2010. Left panels (a, c, and e) are for 6 a.m. and right panels (b, d, and f) are for 6 p.m.

structure in the data of interest. Thus, it is widely used to objectively characterize the dominant spatial and temporal patterns of climate variability [26]. Figure 6 shows the first EOF mode of LST anomalies in the morning by season. Its spatial pattern largely resembles that of the standard deviation and explains 72% (SON) to 86% (DJF) of the total variance, suggesting that the variance of the LST anomalies is dominated by a large-scale coherent pattern. The temporal variation of the EOF1, the first principle component (PC1), resembles that of the ENSO. Thus, the anomalies of morning LST are dominated by El Niño (1997-1998)—more so during the MAM and DJF seasons than during the JJA and SON

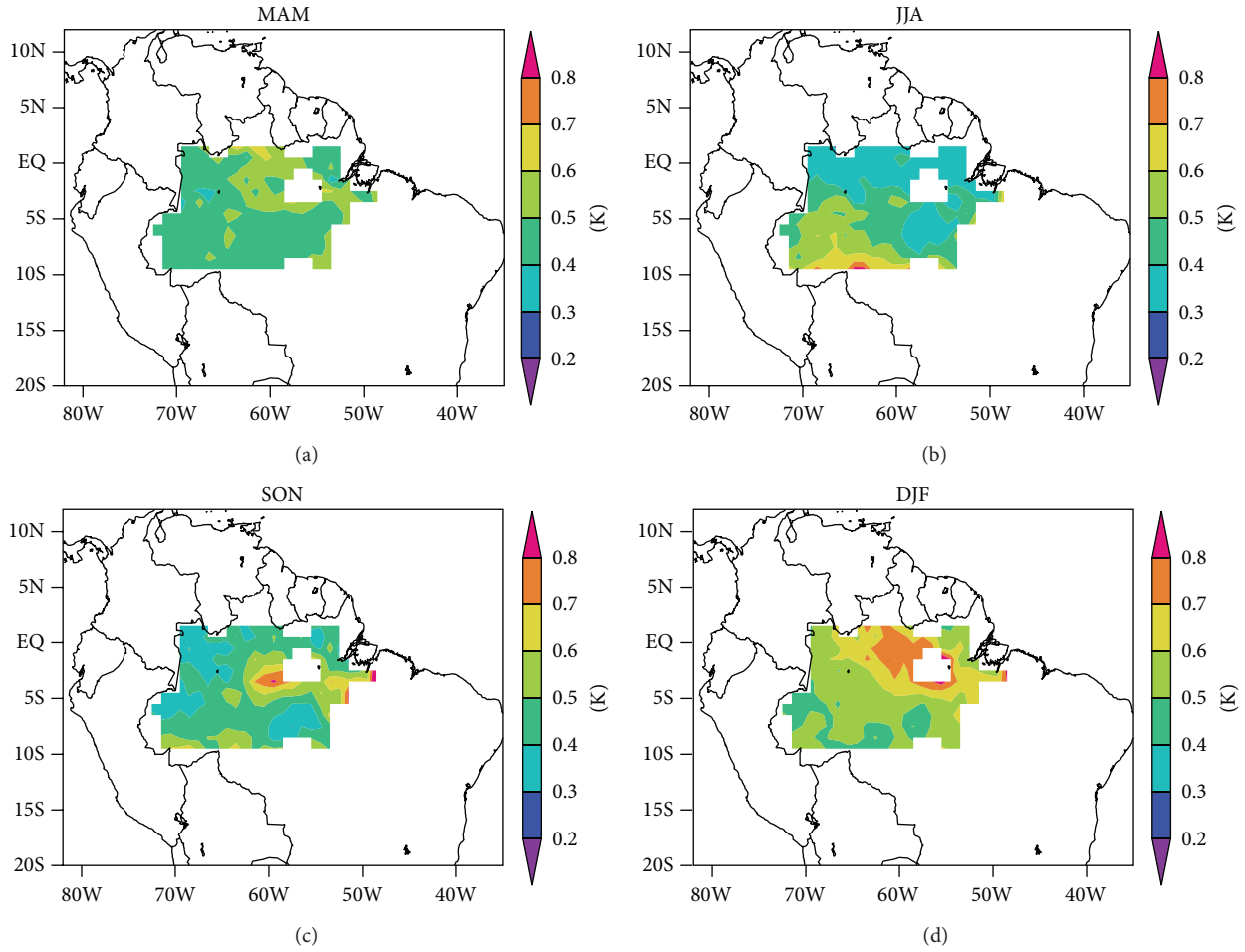

Figure 4: Standard deviation of the remotely sensed LST anomalies at 6:30 a.m. over Amazon rainforests for the following seasons: (a) MAM, (b) JJA, (c) SON, and (d) DJF.

Table 1: Correlation coefficient between EOF patterns (for the Amazon rainforests).

	MAM	JJA	SON	DJF
LST a.m. versus p.m.	0.7	0.68	−0.27	0.54
Rain versus LST a.m.	0.5	−0.04	0.25	−0.08
Rain versus LST p.m.	0.56	−0.05	−0.59	0.19

seasons. Such a seasonal dependence of LST variation is associated with a stronger influence of El Niño on rainfall and cloudiness (e.g., [8]).

The relationship between morning and afternoon LST anomalies can be used to infer their causes. For example, humid and rainy conditions would reduce longwave cooling and increase morning LST anomalies but will also increase evapotranspiration and thus reduce afternoon LST anomalies. Therefore, we would expect a negative correlation between the morning and afternoon LST anomalies. On the other hand, cold front incursions during the dry season could reduce both morning and afternoon LST [27, 28], leading to a positive correlation. Table 1 shows the correlations of the EOF1 spatial patterns by season among three data sources: morning LST anomalies, afternoon LST anomalies, and rainfall anomalies.

4. Results over the Congo Basin Rainforest

The rainforests of Africa are mostly found in the Congo River basin on the Atlantic side of the continent. Thus we choose the domain of 10°E, −5°S to 30°E, 5°S for this study.

Figure 7 shows that there is a clear relationship between the domain averaged LST anomalies at 6:30 p.m. and the 6-month SPI over the Congo basin during the wet season. This negative correlation is reasonable because LST anomalies are more influenced by the cloud solar effect in daytime during the wet season.

The spatial patterns of the LST anomaly interannual variations for different seasons are shown in Figures 8 and 9. This variation is less during the rainy season (usually November to March) and larger during the dry season (usually April to October). This is presumably due to a greater sensitivity of the LST anomalies to changes of atmospheric humidity, cloudiness, and rainfall when the atmosphere and soil are less saturated. The variation is larger at sunset (afternoon) than

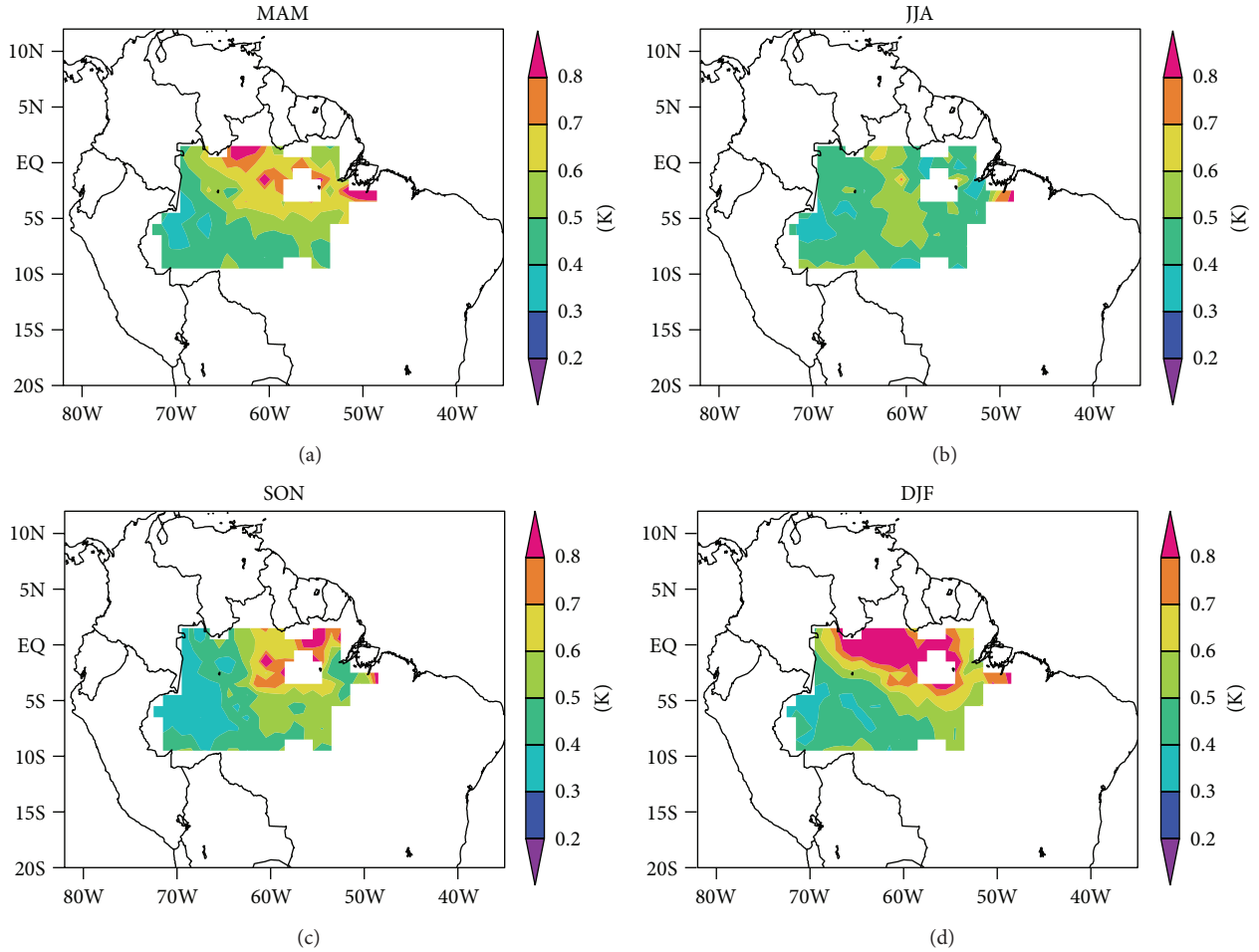

Figure 5: The same as Figure 4 but at 6:30 p.m.

at sunrise (morning), in agreement with observations of the diurnal cycle of temperature over the region [29].

Figure 10 shows the first EOF of SSM/I LST anomalies at 6:30 a.m. over the Congo basin. Its patterns are dominated by a north-south gradient in MAM and DJF. These patterns are directly related to the patterns of African monsoon rainfall variability. For instance, in JJA (boreal summer) the negative EOF values propagate from west to east with attenuation, which is consistent (in trend) with the extension of the precipitation zone from the east Atlantic. In DJF (austral summer), the EOF is clearly layered from north to south—with the precipitation zone occurring over the southern part of the continent, centered around 10°S latitude [30]. The JJA EOF pattern resembles the southwesterly gradient of the August rainfall in the domain of 10°E, −5°S to 20°E, 5°S [31]. The correlation coefficients between morning EOF and afternoon EOF are 0.29, 0.58, 0.15, and 0.49 for MAM, JJA, SON, and DJF, respectively (notice that they are better correlated when there is little rain (JJA) or near constant rain (DJF)). Low correlations are seen during the rainy seasons (MAM and SON) because of the higher soil moisture (and thus lower sensitivity of the afternoon LST anomalies to rainfall).

5. Summary and Conclusions

Interannual variations of LST anomalies over the tropical rainforests are correlated with variations of SST (e.g., El Niño), with the LST anomalies lag Niño 3.4 by 3-4 months. Of the two tropical forests considered, the Amazon forest is more sensitive to such SST variations than the Congo. Drought, as a consequence of soil moisture deficiency, causes an increase in LST anomalies by reducing the latent heat flux (i.e., evapotranspiration). The stronger drought in 1998 had a much greater impact on LST anomalies than the weaker one in 2005. This result is consistent with the greater drought stress and the increase in fire events seen in 1998 versus 2005 [32]. A previous study has suggested that a dry rainfall anomaly in the western Congo is associated with El Niño, although the influence of it is complicated by the effects of the tropical Atlantic and Indian Ocean SST anomaly [33].

The morning and afternoon observations from SSM/I and SSMIS facilitate the investigation of the interannual changes of LST anomalies on a diurnal basis. In general, the afternoon LST anomalies tend to vary more than the morning LST anomalies. A comparison with NCEP datasets indicates that

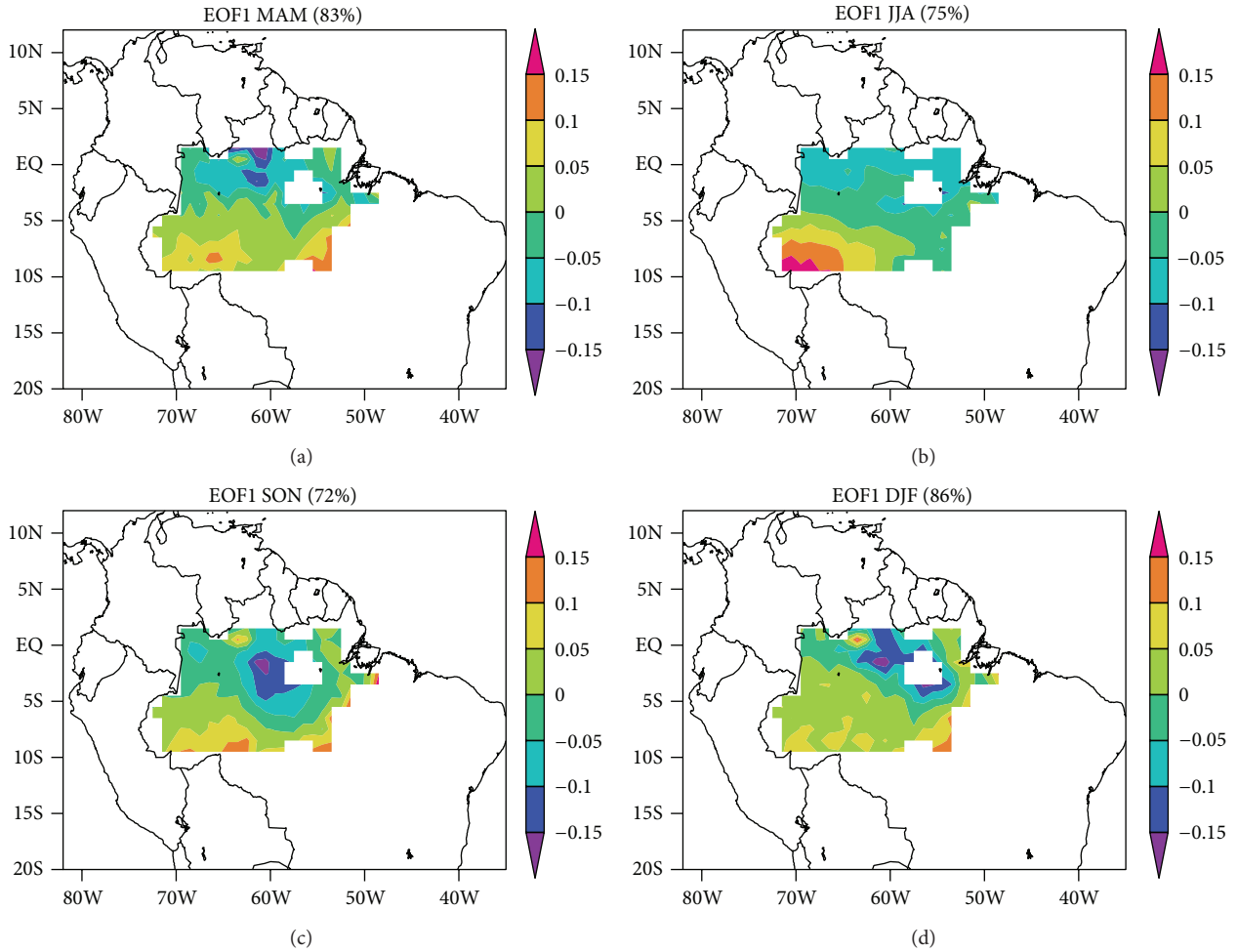

Figure 6: First EOF of the remotely sensed LST anomalies at 6:30 a.m. over Amazon rainforests for the following seasons: (a) MAM, (b) JJA, (c) SON, and (d) DJF.

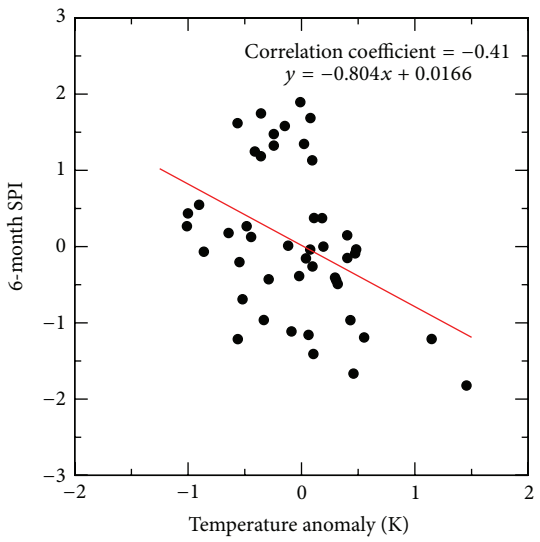

Figure 7: Scatterplot of domain averaged LST anomalies at 6:30 p.m. and 6-month SPI over Congo rainforests during the wet season. The linear trend is determined by a least-square fitting.

the differences between the morning and afternoon remotely sensed temperatures are physically reasonable. The morning LST seems to be controlled by humidity, and it is close to the surface air temperature from NCEP reanalysis.

For both tropical rainforests, the spatial patterns of the morning and afternoon LST anomalies were examined in terms of the standard deviations and EOFs. Change of LST anomalies in the Amazon shows a strong spatial variation, with the largest deltas (of LST anomalies) occurring in the central Amazon. In contrast, changes of LST anomalies in the Congo are more spatially uniform. Variability in both the Amazon and the Congo basins is most pronounced during the wet season—and in the afternoon. This is clearly a result of the variability of cloudiness and its reduction of solar radiation. The first EOF mode explains much of the variance in most of the cases. The LST anomaly spatial patterns during the transitional seasons tend to be less organized than those during the wet and dry seasons.

In conclusion, the SSM/I derived LST product over the tropical forests offers a unique data source for studying land atmosphere interactions. Its analysis shows the differences

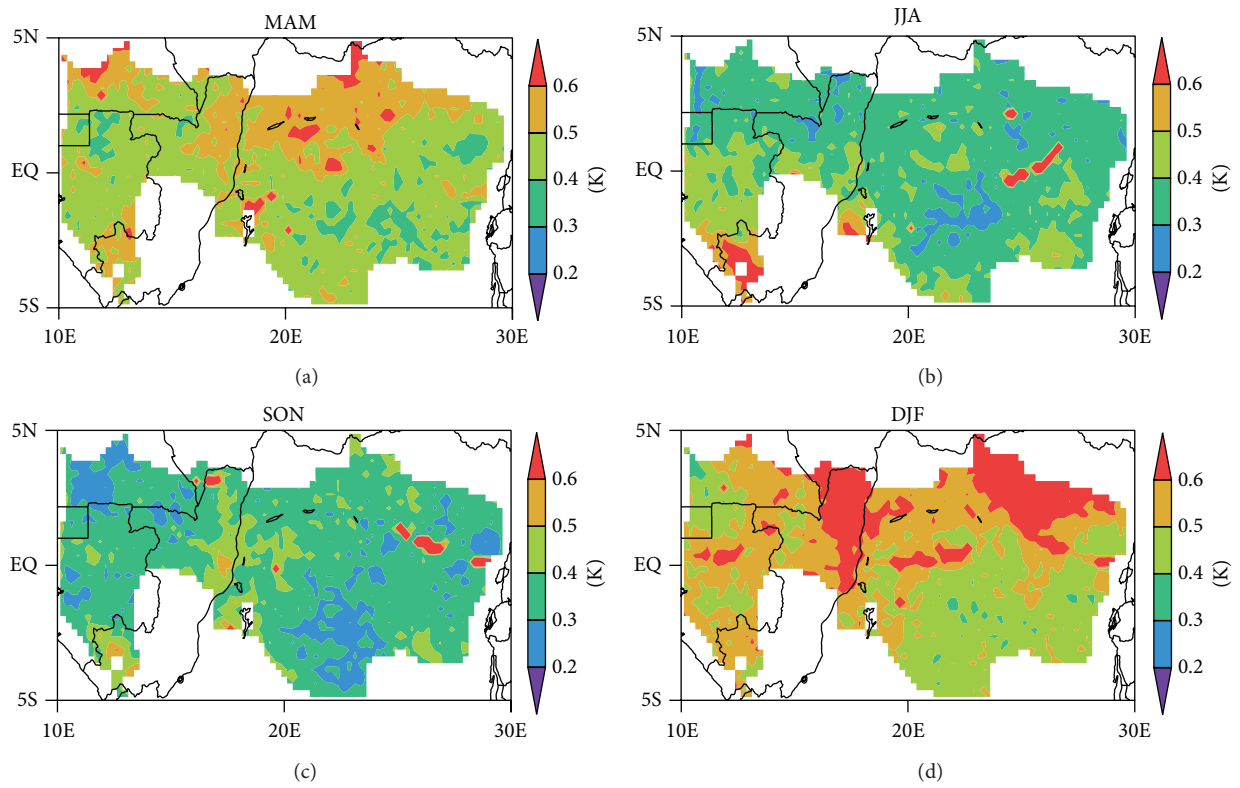

Figure 8: Standard deviation of the remotely sensed LST anomalies at 6:30 a.m. over Congo rainforests for the following seasons: (a) MAM, (b) JJA, (c) SON, and (d) DJF.

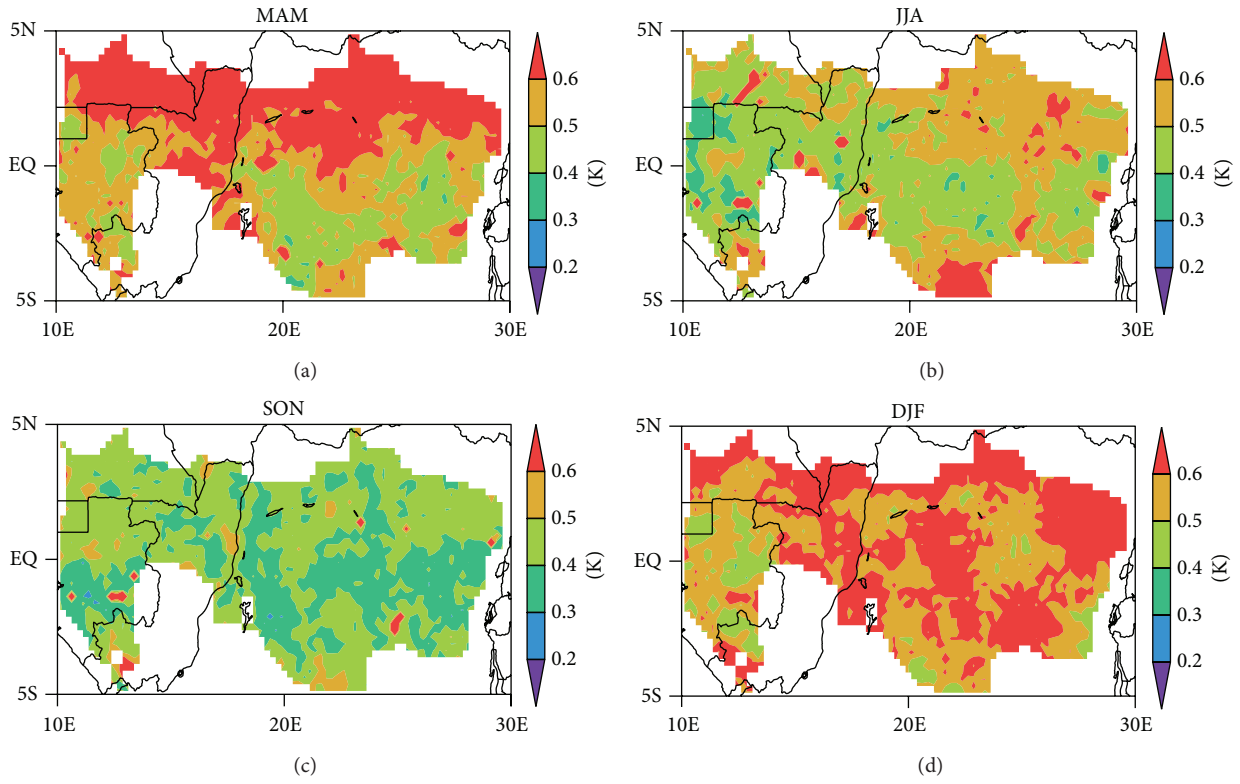

Figure 9: The same as Figure 8 but at 6:30 p.m.

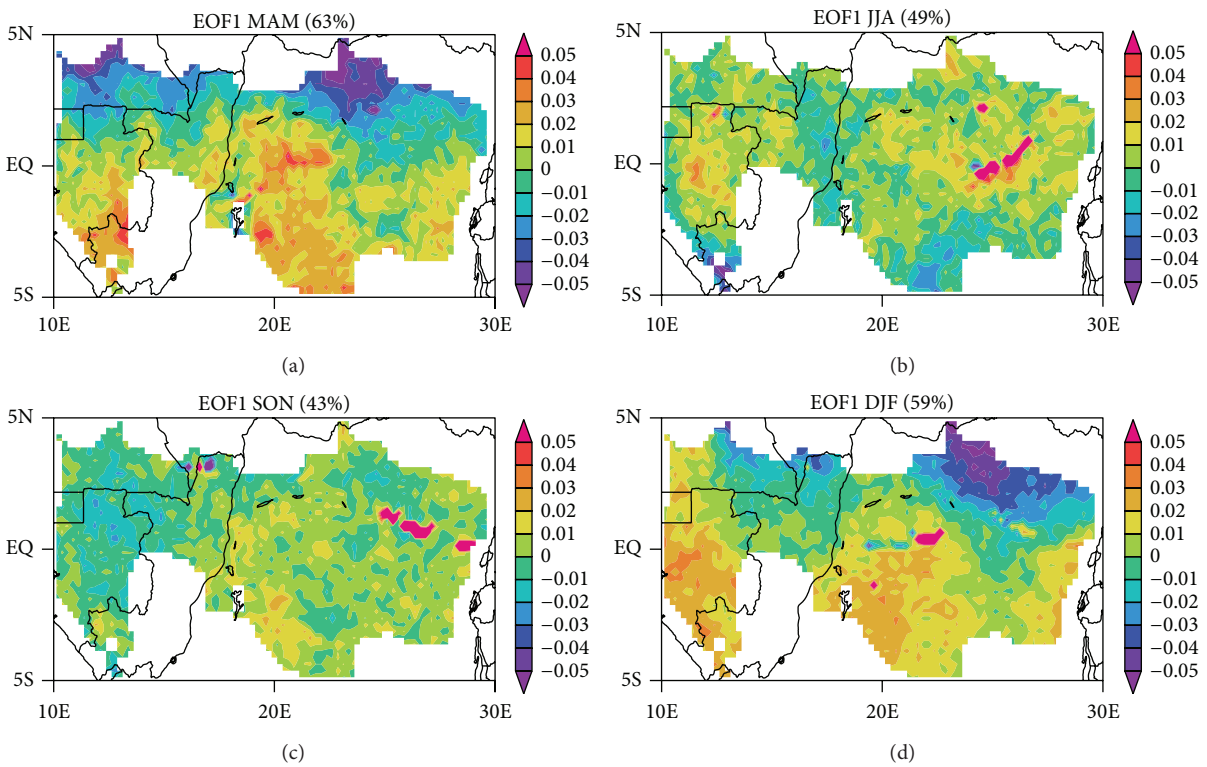

Figure 10: First EOF of the remotely sensed LST anomalies at 6:30 a.m. over Congo rainforests for the following seasons: (a) MAM, (b) JJA, (c) SON, and (d) DJF.

and similarities between morning and afternoon LST and reveals their physical linkages to SST, solar radiation, precipitation, and humidity.

This study contributes to our understanding of the linkage between climate extremes (e.g., drought) and canopy surface temperature. The comparisons between the morning and the afternoon LST anomalies offer a new perspective on land-atmospheric interactions. Since most tropical rainforests suffer from a lack of observational data, this passive microwave based LST dataset can be used for improving estimates from GCMs and hydrological models.

Conflict of Interests

The authors declare that there is no conflict of interests regarding the publication of this paper.

Acknowledgments

This work was supported by startup funds from the Texas A&M University College of Engineering and the Zachry Department of Civil Engineering, the National Science Foundation Grant (AGS-0937400), and DOE GoAmazon DE-SC0011117. It has benefitted from the use of the Texas A&M Supercomputing Facility (http://sc.tamu.edu/). The authors would also like to thank Dr. Chi-Fan Shih at the University Corporation for Atmospheric Research (UCAR) for his assistance with the NCEP data. The open access publishing fees for this paper have been covered by the Texas A&M University Online Access to Knowledge (OAK) Fund, supported by the University Libraries and the Office of the Vice President for Research.

References

[1] M. New, M. Hulme, and P. Jones, "Representing twentieth-century space-time climate variability. Part II: development of 1901-96 monthly grids of terrestrial surface climate," *Journal of Climate*, vol. 13, no. 13, pp. 2217–2238, 2000.

[2] K. E. Trenberth, P. D. Jones, P. Ambenje et al., "Observations: surface and atmospheric climate change," in *Climate Change 2007: The Physical Science Basis*, S. Solomon, D. Qin, M. Manning et al., Eds., Contribution of Working Group I to the Fourth Assessment Report of the Intergovernmental Panel on Climate Change, Cambridge University Press, New York, NY, USA, 2007.

[3] Y. Malhi and J. Wright, "Spatial patterns and recent trends in the climate of tropical rainforest regions," *Philosophical Transactions of the Royal Society B: Biological Sciences*, vol. 359, no. 1443, pp. 311–329, 2004.

[4] A. White, M. G. R. Cannell, and A. D. Friend, "CO_2 stabilization, climate change and the terrestrial carbon sink," *Global Change Biology*, vol. 6, no. 7, pp. 817–833, 2000.

[5] G. L. Vourlitis, N. P. Filho, M. M. S. Hayashi et al., "Effects of meteorological variations on the CO_2 exchange of a Brazilian transitional tropical forest," *Ecological Applications*, vol. 14, no. 4, pp. S89–S100, 2004.

[6] W. Li, P. Zhang, J. Ye, L. Li, and P. A. Baker, "Impact of two different types of El Niño events on the Amazon climate and ecosystem productivity," *Journal of Plant Ecology*, vol. 4, pp. 91–99, 2011.

[7] H. Gao, R. Fu, R. E. Dickinson, and R. I. N. Juárez, "A practical method for retrieving land surface temperature from AMSR-E over the amazon forest," *IEEE Transactions on Geoscience and Remote Sensing*, vol. 46, no. 1, pp. 193–199, 2008.

[8] P. A. Arias, R. Fu, C. D. Hoyos, W. H. Li, and L. M. Zhou, "Changes in cloudiness over the Amazon rainforests during the last two decades: diagnostic and potential causes," *Climate Dynamics*, vol. 37, no. 5, pp. 1151–1164, 2011.

[9] J. Hansen, M. Sato, and R. Ruedy, "Radiative forcing and climate response," *Journal of Geophysical Research D: Atmospheres*, vol. 102, no. 6, pp. 6831–6864, 1997.

[10] S. F. B. Tett, P. A. Stott, M. R. Allen, W. J. Ingram, and J. F. B. Mitchell, "Causes of twentieth-century temperature change near the Earth's surface," *Nature*, vol. 399, no. 6736, pp. 569–572, 1999.

[11] R. L. Armstrong and M. J. Brodzik, "An earth-gridded SSM/I data set for cryospheric studies and global change monitoring," in *Satellite Monitoring of the Earth's Surface and Atmosphere*, pp. 155–163, Pergamon Press, Oxford, UK, 1995.

[12] F. J. Wentz, "User's manual SSM/I antenna temperature tapes," RSS Technical Report 120191, Remote Sensing Systems, Inc., Santa Rosa, Calif, USA, 1993.

[13] B. Rudolf and U. Schneider, "Calculation of gridded precipitation data for the global land-surface using in-situ gauge observations," in *Proceedings of the 2nd Workshop of the International Precipitation Working Group (IPWG '04)*, EUMETSAT, Monterey, Calif, USA, October 2004.

[14] R. I. N. Juarez, M. L. Goulden, R. B. Myneni, R. Fu, S. Bernardes, and H. Gao, "An empirical approach to retrieving monthly evapotranspiration over Amazonia," *International Journal of Remote Sensing*, vol. 29, no. 24, pp. 7045–7063, 2008.

[15] T. B. Mckee, N. J. Doesken, and J. Kleist, "The relationship of drought frequency and duration to times scales," in *Proceedings of the 8th Conference on Applied Climatology*, pp. 179–184, Anaheim, Calif, USA, January 1993.

[16] World Meteorological Organization, "WMO: standardised verification system for long-range forecasts," in *Manual on the Global Data-Processing System*, WMO no. 485, World Meteorological Organization, Geneva, Switzerland, 2012.

[17] D. S. Pai, L. Sridhar, P. Guhathakurta, and H. R. Hatwar, "District-wide drought climatology of the southwest monsoon season over India based on standardized precipitation index (SPI)," *Natural Hazards*, vol. 59, no. 3, pp. 1797–1813, 2011.

[18] N. Subash and H. S. R. Mohan, "Trend detection in rainfall and evaluation of standardized precipitation index as a drought assessment index for rice-wheat productivity over IGR in India," *International Journal of Climatology*, vol. 31, no. 11, pp. 1694–1709, 2011.

[19] S. M. Vicente-Serrano, S. Beguería, and J. I. López-Moreno, "A multiscalar drought index sensitive to global warming: the standardized precipitation evapotranspiration index," *Journal of Climate*, vol. 23, no. 7, pp. 1696–1718, 2010.

[20] W. Li, R. Fu, R. I. N. Juárez, and K. Fernandes, "Observed change of the standardized precipitation index, its potential cause and implications to future climate change in the Amazon region," *Philosophical Transactions of the Royal Society B: Biological Sciences*, vol. 363, no. 1498, pp. 1767–1772, 2008.

[21] E. Kalnay, M. Kanamitsu, R. Kistler et al., "The NCEP/NCAR 40-year reanalysis project," *Bulletin of the American Meteorological Society*, vol. 77, no. 3, pp. 437–471, 1996.

[22] A. K. Betts, "Coupling of water vapor convergence, clouds, precipitation, and land-surface processes," *Journal of Geophysical Research D: Atmospheres*, vol. 112, no. 10, Article ID D10108, 2007.

[23] H. J. I. Rinne, A. B. Guenther, J. P. Greenberg, and P. C. Harley, "Isoprene and monoterpene fluxes measured above Amazonian rainforest and their dependence on light and temperature," *Atmospheric Environment*, vol. 36, no. 14, pp. 2421–2426, 2002.

[24] K. E. Trenberth, "The definition of El Niño," *Bulletin of the American Meteorological Society*, vol. 78, no. 12, pp. 2771–2777, 1997.

[25] K. E. Trenberth, J. M. Caron, D. P. Stepaniak, and S. Worley, "Evolution of el niño-Southern Oscillation and global atmospheric surface temperatures," *Journal of Geophysical Research D: Atmospheres*, vol. 107, no. 8, pp. AAC 5-1–AAC 5-17, 2002.

[26] E. N. Lorenz, "Empirical orthogonal functions and statistical weather prediction," Scientific Report 1, Statistical Forecasting Project, MIT, Department of Meteorology, Cambridge, Mass, USA, 1956.

[27] W. Li and R. Fu, "Influence of cold air intrusions on the wet season onset over Amazonia," *Journal of Climate*, vol. 19, no. 1, pp. 257–275, 2006.

[28] R. Fu, L. Yin, W. Li et al., "Increased dry-season length over southern Amazonia in recent decades and its implication for future climate projection," *Proceedings of the National Academy of Sciences of the United States of America*, vol. 110, no. 45, pp. 18110–18115, 2013.

[29] C. B. Biona, A. Druilhet, B. Benech, and R. Lyra, "Diurnal cycle of temperature and wind fluctuations within an African equatorial rain forest," *Agricultural and Forest Meteorology*, vol. 109, no. 2, pp. 135–141, 2001.

[30] S. Gadgil and S. Sajani, "Monsoon precipitation in the AMIP runs," *Climate Dynamics*, vol. 14, no. 9, pp. 659–689, 1998.

[31] S. E. Nicholson, "The intensity, location and structure of the tropical rainbelt over west Africa as factors in interannual variability," *International Journal of Climatology*, vol. 28, no. 13, pp. 1775–1785, 2008.

[32] L. E. O. C. Aragão, Y. Malhi, N. Barbier et al., "Interactions between rainfall, deforestation and fires during recent years in the Brazilian Amazonia," *Philosophical Transactions of the Royal Society B: Biological Sciences*, vol. 363, no. 1498, pp. 1779–1785, 2008.

[33] S. E. Nicholson and A. K. Dezfuli, "The relationship of rainfall variability in western equatorial Africa to the tropical oceans and atmospheric circulation. Part I: the boreal spring," *Journal of Climate*, vol. 26, no. 1, pp. 45–65, 2013.